J. Membrane Biol. 113, 261–268 (1990)

The Journal of
Membrane Biology

Novel Type of Ion Channel Activated By Pb^{2+}, Cd^{2+}, and Al^{3+} in Cultured Mouse Neuroblastoma Cells

M. Oortgiesen, R.G.D.M. van Kleef, and H.P.M. Vijverberg
Research Institute of Toxicology, University of Utrecht, NL-3508 TD Utrecht, The Netherlands

Summary. Superfusion with Pb^{2+} induces a slow, noninactivating and reversible inward current in voltage-clamped N1E-115 neuroblastoma cells. The amplitude of this inward current increases in the range of 1–200 μM Pb^{2+}. Single-channel patch-clamp experiments have revealed that this inward current is mediated by discrete ion channels. Reversal potentials from linear *I–V* relationships are close to 0 mV for whole-cell and single-channel currents and the single-channel conductance amounts to 24 pS. The Pb^{2+}-induced membrane current is not mediated by various known types of ion channels, since it is not blocked by external tetrodotoxin, tetraethylammonium, D-tubocurarine, atropine, ICS 205-930 and by internal EGTA. In Na^+-free solutions superfusion with Pb^{2+} neither evokes a whole-cell inward current, nor single-channel openings. At −80 mV the open-time distribution of the single channels activated by 1 μM Pb^{2+} is dual exponential with time constants of 17 and 194 msec. When the Pb^{2+} concentration is increased from 1 to 20 μM these time constants decrease to 2 and 13 msec, but the amplitude of single-channel currents remains −1.9 nA. Cd^{2+} and Al^{3+} induce inward currents and single-channel openings similar to Pb^{2+}. Time constants fitted to the open-time distribution of single channels are 14 and 135 msec in the presence of 1 μM Cd^{2+} and 15 and 99 msec in the presence of 50 μM Al^{3+}. Conversely, Cu^{2+} induces an irreversible inward current in neuroblastoma cells. Single-channel openings are undetected in the presence of Cu^{2+} and in Na^+-free solutions Cu^{2+} is still able to induce an inward current. It is concluded that Pb^{2+}, Cd^{2+} and possibly Al^{3+} activate a novel type of metal ion-activated (MIA) channel in N1E-115 cells.

Key Words neuroblastoma cell · voltage clamp · single-channel current · heavy metal · lead · cadmium · aluminum · copper

Introduction

Various metal ions interfere with membrane functions that are normally regulated by Ca^{2+}. Elevation of the internal Ca^{2+} concentration may cause activation of K^+- and Cl^--selective, as well as nonselective cation channels in different cell types (for reviews *see*, Owen, Segal & Barker, 1986; Blatz & Magleby, 1987; Partridge & Swandulla, 1988). Some metal ion species are known to permeate through voltage-dependent Ca^{2+} channels, whereas others block Ca^{2+} currents and are widely used as inorganic Ca^{2+} antagonists (Hagiwara & Byerly, 1981). Injection of a range of metal ions into molluscan neurones has demonstrated that certain ion species only are able to induce an outward K^+ current, which is very similar to the Ca^{2+}-activated K^+ current (Gorman & Hermann, 1979). In addition, an inward current, which is supposed to be mediated by nonselective cation channels, has been observed in molluscan neurones after external application of high concentrations of Cu^{2+} (Weinreich & Wonderlin, 1987). In human erythrocytes, internal Pb^{2+} has been shown to activate Ca^{2+}-dependent K^+ channels, but also to block these channels at high concentrations (Shields et al., 1985).

In N1E-115 neuroblastoma cells a Ca^{2+}-activated, nonspecific cation channel and two types of Ca^{2+}-activated K^+ current have been characterized (Yellen, 1982; Romey et al., 1984; Quandt, 1988). Blocking effects of metal ions on two types of voltage-dependent Ca^{2+} current have been described in detail (Narahashi, Tsunoo & Yoshii, 1987). Recently, we have reported that in N1E-115 cells nanomolar concentrations of Pb^{2+} block the nicotinic receptor-mediated inward current, whereas voltage-dependent Ca^{2+} channels are blocked in the micromolar range. In the course of this study an inward current induced by concentrations of Pb^{2+} higher than 1 μM was discovered (Oortgiesen et al., 1989).

The present study provides a more detailed description of the Pb^{2+}-induced inward current in voltage-clamped neuroblastoma cells and outside-out membrane patches. In addition, the effects of Pb^{2+} and those of Cd^{2+}, Al^{3+} and Cu^{2+} are compared.

Materials and Methods

Mouse neuroblastoma cells of the clone N1E-115 (Amano, Richelson & Nirenberg, 1972) were grown in Dulbecco's modi-

fied Eagle medium supplemented with 7.5% fetal calf serum and the following amino acids (in mM): L-cysteine · HCl 0.3, L-alanine 0.4, L-asparagine 0.45, L-aspartic acid 0.4, L-proline 0.4 and L-glutamic acid 0.4. The cultures were maintained at 37°C in a humidified atmosphere containing 5% CO_2. Cells of passages 30–45 were subcultured in 35-mm plastic tissue culture dishes. Cell differentiation was initiated 2–3 days later by adding 1 mM N^6, 2′-O-dibutyryladenosine 3′:5′-cyclic monophosphate and 1 mM 3-isobutyl-1-methylxanthine to the culture medium. This medium was refreshed every 2–3 days. Cells were used for experiments 6–12 days after induction of differentiation.

Experiments were carried out using whole-cell voltage clamp and single-channel patch-clamp techniques (Hamill et al., 1981). The resistance of fire polished glass pipettes was 3–5 MΩ in whole-cell voltage-clamp experiments and 5–8 MΩ in patch-clamp experiments. The liquid junction potential at the tip of the electrode was compensated before each experiment and remained constant within 1 mV. During whole-cell voltage-clamp experiments the series conductance of approximately 0.15 μS was compensated for 60–70%. The membrane potential was held at −80 mV unless otherwise stated. The recordings were low-pass filtered (−3 dB at 1 kHz; 12 dB/octave), digitized by a transient recorder (8 bits; 1024 points/record) and stored on magnetic disc for off-line computer analysis.

Transitions between open and closed states of the single ion channels were identified using 50% of the open-channel amplitude as threshold criterion. The probability of channels being open was determined as the ratio between the time spent in the open configuration by all channels and the total recording time:

$$P_{ot} = (\Sigma n_{open} \cdot t)/t_{total}. \quad (1)$$

Open-time histograms were obtained from records containing only single channel openings. When more than three channels were open simultaneously, the patch was excluded from kinetic analysis. The channel open times were divided into classes of approximately equal frequency and are presented in frequency density histograms (Bendat & Piersol, 1971). Time constants and SD's were estimated by a nonlinear least-squares exponential algorithm (Marquardt, 1963). Results were compared using a two-tailed Student's t test (Diem & Lentner, 1968).

The control external solution contained (in mM): NaCl 125, KCl 5.5, $CaCl_2$ 1.8, $MgCl_2$ 0.8, HEPES 20, glucose 25 and sucrose 36.5. The pH was adjusted to 7.3 with approximately 10 mM NaOH. In some experiments nitrate salts instead of chloride salts were used. To compensate for osmolality changes that occurred when high concentrations of metal salts were added, the sucrose concentration of the external solution was reduced. The pipette solution contained (in mM): KCl 150, NaCl 10, HEPES 10 and $MgCl_2$ 1. The pH was adjusted to 7.2 with approximately 3 mM KOH. In whole-cell voltage-clamp experiments ion channels were activated by direct, whole-cell superfusion with known concentrations of the metal for adjustable periods using a servomotor operated valve (Neijt, te Duits & Vijverberg, 1988). In patch-clamp experiments ion channels were activated by addition of the metals to the bathing solution. The concentration of heavy metal ions contaminating the control external solution was less than 130 nM as calculated from the data supplied with the chemicals used. All experiments were carried out at room temperature (20–24°C).

$Pb(NO_3)_2$, $Cu(NO_3)_2$, $Cd(NO_3)_2$ and $Al(NO_3)_3$ were obtained from Fluka Chemie AG, Buchs, Switzerland; tetraethylammonium chloride (TEA), tetrodotoxin (TTX) and ouabain from Sigma, St. Louis, MO; D-tubocurarine chloride (DTC) from Boroughs Wellcome, London, UK; atropine sulphate from OPG, Utrecht, The Netherlands. ICS 205-930 (3α-tropanyl-1H-indole-3-carboxylic acid ester) was donated by Sandoz, Basel, Switzerland.

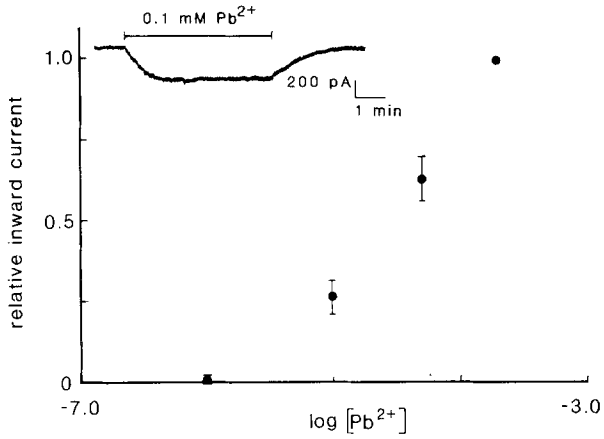

Fig. 1. Concentration dependence of the inward current induced by superfusion of Pb^{2+} in whole-cell voltage-clamped neuroblastoma cells. During superfusion with 100 μM Pb^{2+} a noninactivating inward current appeared that reversed upon washing with control external solution (*see* inset, superfusion period is indicated by bar). The relative inward current (ordinate) was calculated by normalizing for each cell the amplitude of the inward current at various concentrations of Pb^{2+} to the value obtained at 200 μM Pb^{2+}. The amplitude of the 200 μM Pb^{2+}-induced inward current varied between cells and ranged from 0.8–14 nA (n = 4). Membrane potential was held at −80 mV

Results

Inward Currents Induced by Pb^{2+}, Cd^{2+} and Al^{3+}

During whole-cell superfusion with Pb^{2+} a noninactivating inward current was observed in cells voltage clamped at a membrane potential of −80 mV. During washing with control external solution the inward current decayed to the control level. The amplitude of the Pb^{2+}-induced inward current increased between 1 and 200 μM Pb^{2+} in a concentration-dependent way (Fig. 1). Further elevation of the Pb^{2+} concentration was impossible, due to the limited solubility of $Pb(NO_3)_2$ in the external solution. The amplitude of the inward current induced by 200 μM Pb^{2+} varied from 0.8–14 nA in four different cells.

In order to elucidate the nature of the Pb^{2+}-induced inward current, the effects of antagonists of various known types of ion channels were examined. The inward current induced by 100 μM Pb^{2+} was neither blocked by 1 μM of the Na^+ channel

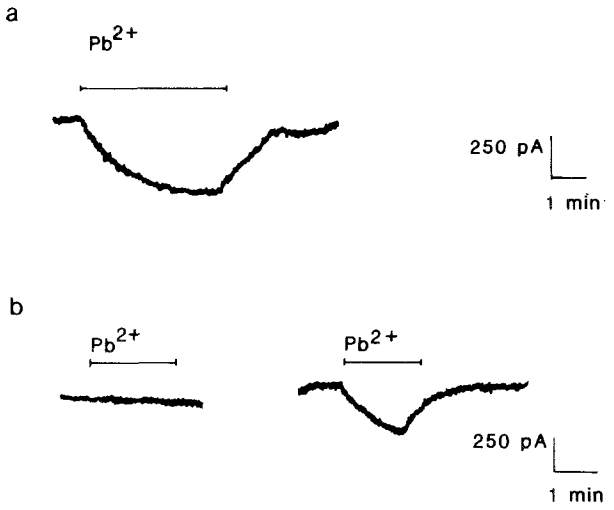

Fig. 2. (*a*) Inward current induced by superfusion with 200 μM Pb^{2+}, while 2 mM Mg-EGTA was present in the pipette solution. (*b*) Absence of current during superfusion with 100 μM Pb^{2+} after replacing all Na^+ with K^+ in the external and the pipette solution (left). In the same cell 100 μM Pb^{2+} induced a marked inward current when superfused with Pb^{2+} in normal external solution (right). Note a slight shift in the holding current due to the different composition of the external solutions. Superfusion periods are indicated by bars. Membrane potential was held at −80 mV

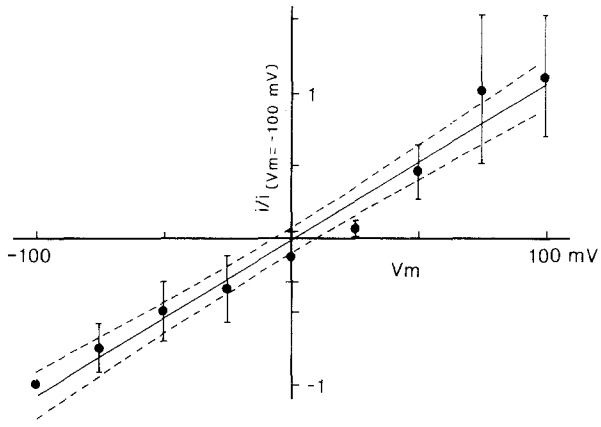

Fig. 3. *I-V* relationship of the 100 μM Pb^{2+}-induced inward current obtained by applying an 8-sec ramp from −100 – +100 mV. Control current records were subtracted from records obtained during the steady Pb^{2+}-induced inward current. Current values, measured at 1-sec (25-mV) intervals, were normalized to the value at the start of the ramp (−100 mV) for each cell. The inward current at −80 mV amounted to 0.7 ± 0.4 nA (n = 4). Depicted are mean normalized values ± SD. Regression analysis showed no deviation of the *I-V* relationship from linearity (P = 0.36). The reversal potential was 0.0 ± 7.3 mV

blocker TTX, nor by 10 mM of the K^+ channel blocker TEA. The inward current was also observed in the presence of 10 μM of the nicotinic antagonist DTC, 1 μM of the muscarinic antagonist atropine and of 0.5 μM of the serotonin 5-HT_3 antagonist ICS 205-930. A possible interaction of externally applied Pb^{2+} with intracellular sites was examined using a pipette solution to which 2 mM Mg-EGTA was added. In the presence of the chelator a normal Pb^{2+}-induced inward current was observed (Fig. 2*a*). Replacement of chloride salts by nitrate salts in the external and the pipette solution also did not abolish the Pb^{2+}-induced inward current. However, when Na^+ was replaced by K^+ in both the external and the pipette solution, an inward current was not detected during superfusion with 100 μM Pb^{2+}, while in the same cell 100 μM Pb^{2+} clearly induced an inward current after changing to normal external solution (Fig. 2*b*). In order to examine whether Pb^{2+} caused impairment of the Na^+/K^+ pump, the effect of ouabain was also investigated. The Pb^{2+}-induced inward current was not blocked in the presence of 3 mM ouabain.

The effect of membrane potential on the Pb^{2+}-induced inward current was studied by ramp stimulation (−100 – +100 mV in 8 sec) in voltage-clamp experiments. Control current records were subtracted from records obtained during the steady Pb^{2+}-induced inward current. Possible contributions of voltage-dependent ion channels to the resulting whole-cell current, that could originate from an interaction of Pb^{2+} with these channels, were excluded by addition of 3 mM TEA and 0.5 μM TTX to the external solution and by replacement of K^+ by Cs^+ in the pipette solution. The amplitude of the Pb^{2+}-induced inward current at −80 mV amounted to 0.7 ± 0.4 nA (n = 4). The *I-V* relationship shown in Fig. 3 was obtained by normalizing the current to the value at the start of the ramp (−100 mV) for each cell and by plotting the mean normalized values and the respective SD at 1-sec (25-mV) intervals. Regression analysis showed no deviation of the *I-V* relationship from linearity (P = 0.36). The reversal potential was 0.0 ± 7.3 mV (n = 4).

Superfusion with Al^{3+} and Cd^{2+} also evoked reversible, noninactivating inward currents. Inward currents induced by superfusion of the same cell with 100 μM Pb^{2+} and 100 μM Cd^{2+} had a similar amplitude and time course (Fig. 4*a*). At the same concentration Al^{3+} induced a two to threefold smaller inward current than Pb^{2+} (Fig. 4*b*). The amplitude of the Cd^{2+}-induced inward current increased with increasing concentrations of Cd^{2+} between 0.1 μM and 10 mM in six cells (Fig. 4*c*). For each cell relative inward currents were obtained by normalizing the amplitudes to the value obtained with 1 mM Cd^{2+}. The mean amplitude of the inward current induced by 1 mM Cd^{2+} amounted to 0.7 ± 0.5 nA (n = 6). Following superfusion with Cd^{2+} at

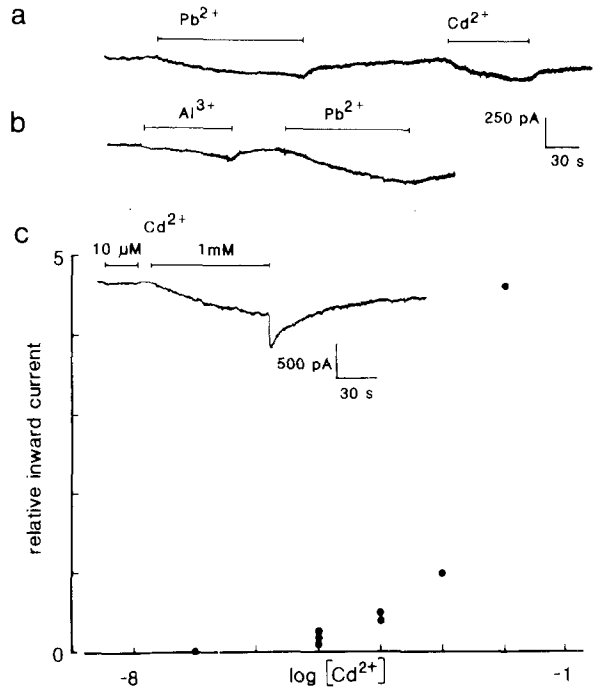

Fig. 4. (*a*) Inward currents induced by superfusion with 100 μM Pb^{2+} and 100 μM Cd^{2+} in the same cell. (*b*) Inward currents induced by superfusion with 100 μM Al^{3+} and 100 μM Pb^{2+} in the same cell. (*c*) Concentration dependence of the inward current induced by superfusion with 0.1–10 mM Cd^{2+}. The relative inward current was calculated by normalizing the amplitude of the inward current at various concentrations of Cd^{2+} to the value obtained at 1 mM Cd^{2+} for each cell. The inset shows inward currents induced by 10 μM and 1 mM Cd^{2+} in the same cell. After superfusion with 1 mM Cd^{2+} a transient increase of the inward current appeared upon washing. Superfusion periods are indicated by bars. Membrane potential was held at −80 mV

concentrations ≥1 mM, a pronounced increase of the inward current was observed upon washing. During continued washing the inward current slowly decayed to the control level (Fig. 4*c* inset).

Single Channels Activated by Pb^{2+}, Cd^{2+} and Al^{3+}

In excised outside-out membrane patches of N1E-115 cells 10 μM Pb^{2+} caused the opening of discrete ion channels (Fig. 5*a*). These ion channel openings were no longer observed within 3–4 min after adding Ca-EGTA in a final concentration of 2 mM to the bathing solution (Fig. 5*b*). At −80 mV the amplitude of single-channel currents was 1.85 ± 0.12 pA (n = 8) in the presence of 10 μM Pb^{2+} and 1.94 ± 0.10 pA (n = 4) in the presence of 1 μM Pb^{2+}. These values do not differ significantly (P = 0.26).

The single-channel current amplitude was measured for a range of membrane potentials from −80 to +80 mV in membrane patches obtained from three cells. The *I-V* relationship of single channels is shown in Fig. 5*c*. Regression analysis did not reveal deviation from linearity (P = 0.70) and the slope of the regression line yielded a single-channel

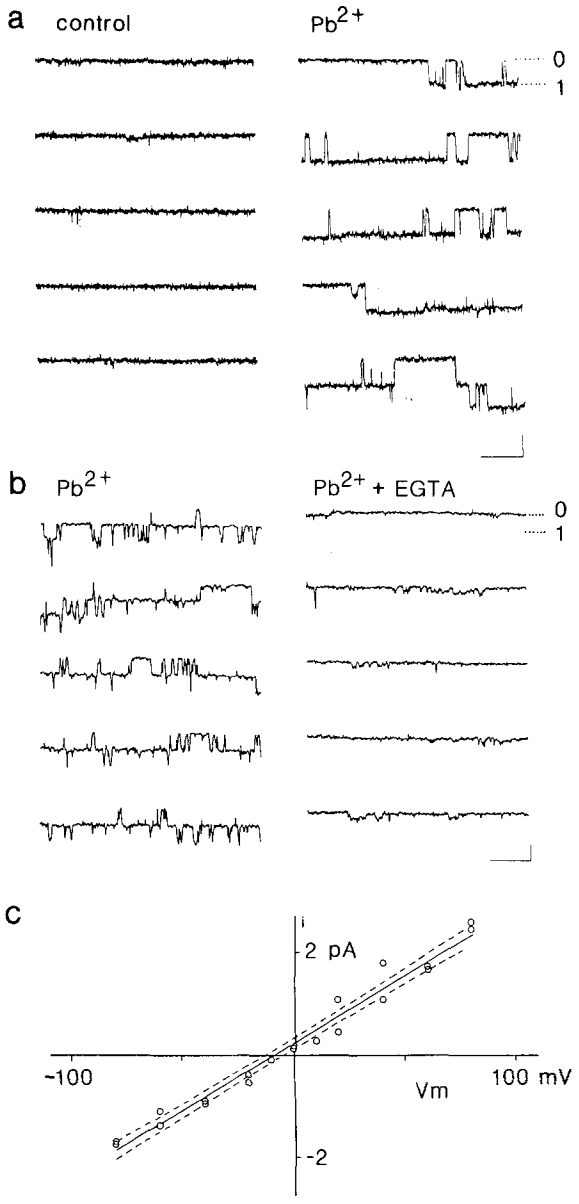

Fig. 5. (*a*) Single-channel openings induced by Pb^{2+}. In normal control solution no channel openings were recorded. After addition of Pb^{2+} to the external solution in a final concentration of 10 μM discrete single-channel openings occurred. (*b*) Multiple single-channel openings induced by 10 μM Pb^{2+} disappear within 3–4 min after addition of 2 mM Ca-EGTA to the bathing solution. Calibration: horizontal 100 msec, vertical 2 pA. (*c*) *I-V* relationship of the Pb^{2+}-activated single channels. Regression analysis showed no deviation of the *I-V* relationship from linearity (P = 0.70). The reversal potential was to −6.1 ± 5.8 mV (n = 3)

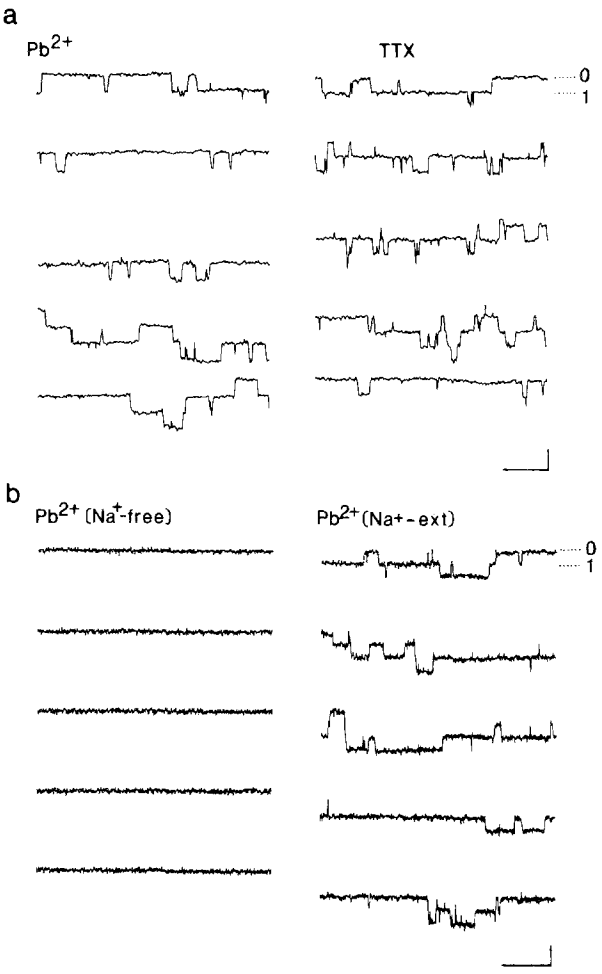

Fig. 6. (*a*) Multiple single-channel openings induced by 10 μM Pb^{2+} in normal external solution (left) and in the presence of 1 μM TTX (right). (*b*) No single-channel openings appeared in the presence of 20 μM Pb^{2+} after replacing all Na^+ with K^+ in the external and in the pipette solution (left). Immediately after changing to a 50% Na^+ external solution single-channel openings appeared (right). In both the external and the pipette solution nitrate salts were used instead of chloride salts. Calibration: horizontal 100 msec, vertical 2 pA

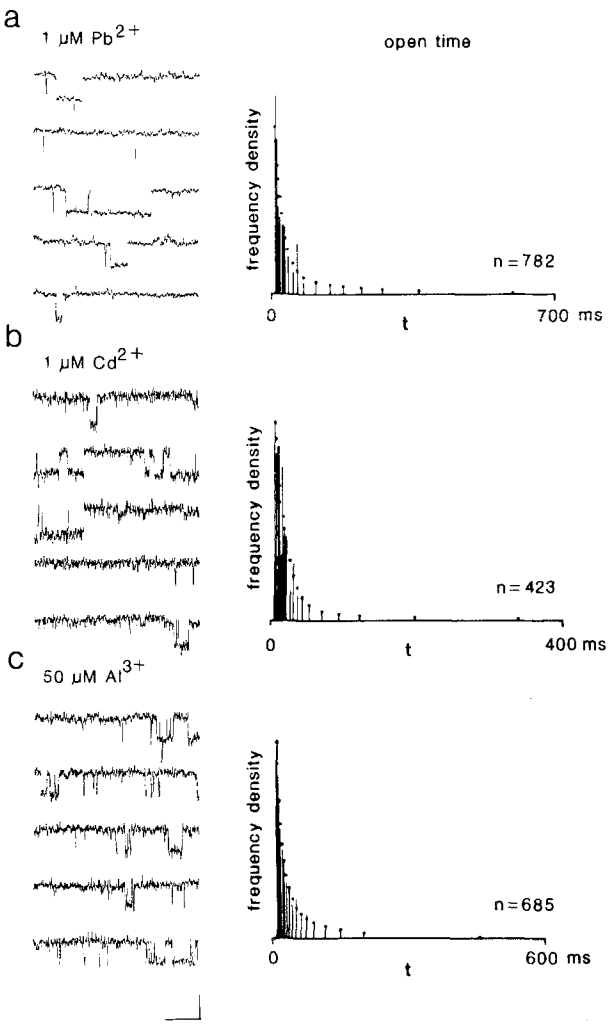

Fig. 7. Single-channel currents induced by (*a*) 1 μM Pb^{2+}, (*b*) 1 μM Cd^{2+} and (*c*) 50 μM Al^{3+} and open-time frequency density histograms. The parameters obtained from the fitted dual-exponential functions, indicated by dots in histogram, are presented in the Table. The Chi-square (degrees of freedom) and the *P* values were 12.3 (15) and 0.66, respectively, in the presence of 1 μM Pb^{2+}; 12.7 (14) and 0.55 in the presence of 1 μM Cd^{2+}; and 8.0 (13) and 0.85 in the presence of 50 μM Al^{3+}. Calibration: horizontal 200 msec, vertical 2 pA

conductance of 24 pS with 95% confidence limits of 1.8 pS. The mean reversal potential of the single-channel current was -6.1 ± 5.8 mV ($n = 3$), which is not significantly different from the reversal potential of the whole-cell Pb^{2+}-induced current ($P = 0.29$).

Similar to whole-cell currents, Pb^{2+}-activated single channels were neither blocked by 1 μM TTX (Fig. 6*a*), 10 mM TEA, nor by replacement of all chloride salts by nitrate salts. When Na^+ was replaced by K^+ in both the external and the pipette solution, 20 μM Pb^{2+} failed to induce single-channel openings. However, immediately upon changing to a 50% Na^+ external solution, containing 65 mM $NaNO_3$, single-channel openings reappeared (Fig. 6*b*).

Figure 7*a* shows the frequency density histogram of the open times of single channels activated by 1 μM Pb^{2+}. The single-channel open-time distribution was established at different concentrations of Pb^{2+}. The frequency density histograms showed dual-exponential open-time distributions. The two time constants fitted to the open-time distributions were reduced when the Pb^{2+} concentration was increased, but consistent changes in the amplitudes of

Table. Parameters of the dual-exponential function $A_1 \cdot \exp(-t/\tau_1) + A_2 \cdot \exp(-t/\tau_2)$ fitted to the open-time frequency density histograms of ion channels activated by Pb^{2+}, Cd^{2+}, and Al^{3+}

Metal	(μM)	τ_1 (msec)	A_1 (%)	τ_2 (msec)	A_2 (%)
Pb^{2+}	1	17.1 ± 2.6	51 ± 5	194 ± 24	49 ± 5
	10	5.5 ± 0.9	70 ± 8	48.9 ± 6.6	30 ± 5
	20	1.9 ± 0.5	71 ± 14	12.6 ± 3.3	31 ± 8
Cd^{2+}	1	13.6 ± 2.5	71 ± 9	135 ± 48	29 ± 7
Al^{3+}	50	14.8 ± 1.6	58 ± 4	99.4 ± 6.8	42 ± 3

the two kinetic components were not observed. The Table shows that the time constant of the fast component decreased from 17 to 2 msec and that of the slow component from 194 to 13 msec when the Pb^{2+} concentration was increased from 1 to 20 μM. In contrast to the duration of channel openings, the probability of channels being open (P_{ot}, *see* Eq. (1)) became greater at increasing Pb^{2+} concentration. Subsequent addition of 1 and 10 μM Pb^{2+} to two outside-out patches revealed that P_{ot}, measured over 100-sec periods, increased from 0.02 and 0.04 to 0.62 and 0.78, respectively. In a limited number of records obtained at −80 and +80 mV marked changes in channel kinetics were not observed.

Cd^{2+} as well as Al^{3+} also caused single ion channels to open (Fig. 7*b,c*). The amplitude of the single-channel current at −80 mV was 1.75 ± 0.09 pA (n = 3) in the presence of 1 μM Cd^{2+} and 2.19 ± 0.03 pA (n = 3) in the presence of 50 μM Al^{3+}. The Al^{3+}-activated single-channel current was significantly greater than that of Pb^{2+}- and Cd^{2+}-activated channels (P = 0.001 and P = 0.001), whereas the current amplitudes of the latter two types of channels could not be distinguished (P = 0.10). The time constants fitted to the open-time histogram obtained from three patches in the presence of 1 μM Cd^{2+} were 14 and 135 msec and those from three patches in the presence of 50 μM Al^{3+} were 15 and 99 msec (*see* Table).

Effects of Cu^{2+}

During superfusion of voltage-clamped neuroblastoma cells with external solution containing 10–500 μM Cu^{2+} an inward current also developed. The Cu^{2+}-induced inward current slowly increased during continued superfusion with Cu^{2+} without reaching a steady level and could not be reversed by washing with either control or 2 mM EGTA-containing external solution for up to 25 min. The Cu^{2+}-induced inward current was also observed in solutions in which chloride salts were replaced by

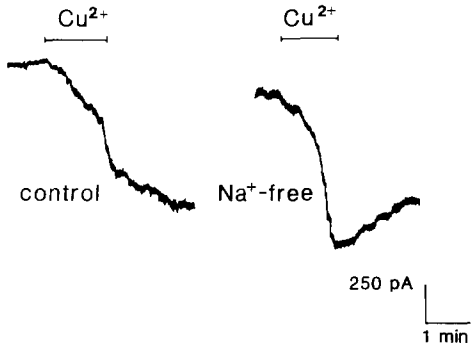

Fig. 8. Inward currents induced by superfusion with 50 μM Cu^{2+} in control external solution (left) and after replacing all Na^+ with K^+ ions in the external solution (right) in the same cell. In all solutions nitrate salts were used instead of chloride salts. Superfusion periods are indicated by horizontal bars. Membrane potential was held at −80 mV

nitrate salts. However, in contrast to Pb^{2+}, Cu^{2+} was able to induce inward currents in Na^+-free solution (Fig. 8). Addition of 30 μM Cu^{2+} to the external solution of excised membrane patches failed to cause discrete single-channel openings, but caused noisy burst-like fluctuations of the membrane current. On subsequent addition of 10 μM Pb^{2+} to the external solution discrete single-channel openings were also observed.

Discussion

A Pb^{2+}-induced inward current in cultured mouse neuroblastoma cells has been characterized in whole-cell voltage-clamp experiments. Further, patch-clamp experiments have revealed that in excised outside-out membrane patches Pb^{2+} activates discrete ion channels. The whole-cell current and the Pb^{2+}-activated ion channels have several properties in common. The whole-cell and the single-channel currents have linear *I-V* relationships with a reversal potential close to 0 mV. The amplitude of the inward current and the probability of single channels being open increase with increasing Pb^{2+} concentration. Moreover, neither a whole-cell current nor single-channel openings can be evoked by Pb^{2+} in Na^+-free solutions. These results indicate that the discrete single-channel currents investigated constitute the Pb^{2+}-induced inward current.

The probability of Pb^{2+}-activated single channels being open (P_{ot}) increased 20–30 fold between 1 and 10 μM Pb^{2+}. This is consistent with the increase of the amplitude of the whole-cell inward current from the detection threshold at 1 μM by at

least 25-fold at 10 μM Pb^{2+} (*see* Fig. 1). It should be noted, however, that both the fast and the slow time constants of the single-channel open-time distribution decreased by a factor of 3–4 in the same concentration range (*see* Table). Therefore, the concentration-dependent increase of the amplitude of the Pb^{2+}-induced current can be explained by a large increase in the frequency of channel opening and a simultaneous, lesser increase of the probability of channel closing.

Properties of the Pb^{2+}-activated channels are distinct from those of presently known types of ion channels in N1E-115 cells. Experiments with selective ion channel blockers, receptor antagonists and with ion substitution indicate that neither voltage-dependent Na^+ and K^+ channels nor acetylcholine and serotonin (5-HT_3) receptor-operated channels are involved. The present results, as well as the finding that the two types of Ca^{2+} current in N1E-115 cells are blocked by Pb^{2+} in the micromolar range (Oortgiesen et al., 1989), indicate that Ca^{2+} channels are not involved. The current-voltage relationship of the Pb^{2+}-induced current is linear with the reversal potential close to 0 mV. Since the pipette solution in reversal potential experiments contained Cs^+ substituted for K^+, the Pb^{2+}-activated ion channel appears permeable to Na^+ as well as Cs^+ and possibly constitutes a nonselective cation channel. Nonselective cation channels activated by internal Ca^{2+} in N1E-115 cells (Yellen, 1982) and Ca^{2+}-activated cation channels in various cell types (Partridge & Swandulla, 1988) have unit conductances and reversal potentials similar to those of the Pb^{2+}-activated ion channels presently described. However, the Ca^{2+}-activated ion channels are blocked by internal EGTA, whereas Pb^{2+}-activated ion channels are not. Therefore, the Na^+-dependent, Pb^{2+}-activated ion channel can be distinguished clearly from ion channels previously characterized in N1E-115 and other types of cells.

Cd^{2+} also induced an inward current, which appears very similar to the Pb^{2+}-induced current with respect to both size and concentration dependence. The amplitudes of the single-channel currents activated by these heavy metal ions cannot be distinguished statistically and the single channels show similar open-time kinetics. These results indicate that Cd^{2+} and Pb^{2+} act on a single, novel type of ion channel, here designated metal ion-activated (MIA) channel. Preliminary observations showed that high concentrations of Cd^{2+} (>100 μM) block Pb^{2+}-activated single channels in a reversible way. Together with the transient increase of the inward current during the removal of high concentrations of Cd^{2+} (*see* Fig. 4*c*, inset), this suggests the presence of a low affinity blocking site at the MIA channel. Low affinity channel block by Pb^{2+} would also explain the marked reduction of the open time of Pb^{2+}-activated channels in the range of 1–20 μM Pb^{2+}. The fast and the slow time constant of the open-time histogram similarly vary with Pb^{2+} concentration (*see* Table) and have been fitted by sigmoidal curves of the type:

$$\tau/\tau_{max} = 1/\{1 + (IC_{50}/[Pb^{2+}])^n\}. \quad (2)$$

The estimated IC_{50} values are 6.6 and 6.1 μM and the slope factors (n) amount to 1.9 and 2.3 for the concentration-effect curve of the fast and the slow time constant, respectively. The result that there is no clear shift from long to short open times with increasing Pb^{2+} concentration and the similarity of the concentration-effect curves indicate that Pb^{2+} equally blocks channels in the short- and the long-lived open state.

Al^{3+} induced smaller inward currents than Pb^{2+} and Cd^{2+}, but the single-channel current amplitude at −80 mV was greater by a significant 10%. It remains unclear whether Al^{3+} activates the same class of MIA channels with modified unit conductance, or activates a distinct class of ion channels. At present, the former hypothesis is preferred, since experiments with Cu^{2+} have shown that MIA channels cannot be activated by any metal ion species.

The inward current induced by Cu^{2+} differs from that induced by the other metal ions, because it was irreversible and because it could be evoked in Na^+-free solutions. In addition, the Cu^{2+}-induced inward current appeared not to be mediated by activation of discrete ion channels. In *Aplysia californica* neurones a similar Cu^{2+}-induced inward current has been reported. This inward current appeared neither to be caused by enhancement of lipid peroxidation nor by impairment of the Na^+/K^+ pump (Weinreich & Wonderlin, 1987).

The MIA channel presently identified can be activated by external application of certain species of metal ions. The nonselective ion channel has a unit conductance of 24 pS, appears to be Na^+-dependent and differs from the various known types of ion channels. Kinetic analysis revealed that the ion channel has at least two open states as well as a resting closed state and a blocked state. The physiological function of the MIA channel remains to be clarified.

The authors wish to acknowledge Ing. A. de Groot for expert technical assistance, Ms. P. Martens for maintaining the cell culture and Prof. J. van den Bercken for his comments on the manuscript. This work was financially supported by Shell Internationale Research Maatschappij B.V.

References

Amano, T., Richelson, E., Nirenberg, P.G. 1972. Neurotransmitter synthesis by neuroblastoma clones. *Proc. Natl. Acad. Sci. USA* **6**:258–263

Bendat, J.S., Piersol, A.G. 1971. Random data: Analysis and measurement procedures. Wiley-Interscience, New York

Blatz, A. L., Magleby, K.L. 1987. Calcium-activated potassium channels. *Trends Neurosci.* **10**:463–467

Diem, K., Lentner, C. 1968. *Wissenschaftliche Tabellen.* Ciba-Geigy AG, Basle

Gorman, A.L.F., Hermann, A. 1979. Internal effects of divalent cations on potassium permeability in molluscan neurones. *J. Physiol. (London)* **296**:393–410

Hagiwara, S., Byerly, L. 1981. Calcium channel. *Annu. Rev. Neurosci.* **4**:69–125

Hamill, O.P., Marty, A., Neher, E., Sakmann, B., Sigworth, F.J. 1981. Improved patch-clamp techniques for high-resolution current recording from cells and cell-free membrane patches. *Pfluegers Arch.* **391**:85–100

Marquardt, D.W. 1963. An algorithm for least-squares estimation of non-linear parameters. *J. Soc. Ind. Appl. Math.* **11**:431–441

Narahashi, T., Tsunoo, A., Yoshii, M. 1987. Characterization of two types of calcium channels in mouse neuroblastoma cells. *J. Physiol. (London)* **383**:231–249

Neijt, H.C., te Duits, I.J., Vijverberg, H.P.M. 1988. Pharmacological characterization of serotonin 5-HT_3 receptor-mediated electrical response in cultured mouse neuroblastoma cells. *Neuropharmacology* **27**:301–307

Oortgiesen, M., Van Kleef, R.G.D.M., Bajnath, R.B., Vijverberg, H.P.M. 1989. Nanomolar concentrations of lead selectively block neuronal nicotinic acetylcholine responses in mouse neuroblastoma cells. *Toxicol. Appl. Pharmacol. (in press)*

Owen, D.G., Segal, M., Barker, J.L. 1986. Voltage-clamp analysis of a Ca^{2+} and voltage-dependent chloride conductance in cultured mouse spinal neurons. *J. Neurophysiol.* **55**:1115–1135

Partridge, L.D., Swandulla, D. 1988. Calcium-activated non-specific cation channels. *Trends Neurosci.* **11**:69–72

Quandt, F.N. 1988. Three kinetically distinct potassium channels in mouse neuroblastoma cells. *J. Physiol. (London)* **395**:401–418

Romey, G., Hugues, M., Schmid-Antomarchi, H., Lazdunski, M. 1984. Apamin: A specific toxin to study a class of Ca^{2+}-dependent K^+ channels. *J. Physiol. (Paris)* **79**:259–264

Shields, M., Grygorczyk, R., Fuhrmann, G.F., Schwarz, W., Passow, H. 1985. Lead-induced activation and inhibition of potassium-selective channels in the human red blood cell. *Biochim. Biophys. Acta* **815**:223–232

Weinreich, D., Wonderlin, W.F. 1987. Copper activates a unique inward current in molluscan neurones. *J. Physiol. (London)* **394**:429–443

Yellen, G. 1982. Single Ca^{2+}-activated nonselective cation channels in neuroblastoma. *Nature (London)* **296**:357–359

Received 28 June 1989; revised 18 September 1989